

# Compartmentalization of metabolic pathways in yeast mitochondria improves the production of branched-chain alcohols

José L Avalos<sup>1,2</sup>, Gerald R Fink<sup>2</sup> & Gregory Stephanopoulos<sup>1</sup>

Efforts to improve the production of a compound of interest in *Saccharomyces cerevisiae* have mainly involved engineering or overexpression of cytoplasmic enzymes. We show that targeting metabolic pathways to mitochondria can increase production compared with overexpression of the enzymes involved in the same pathways in the cytoplasm. Compartmentalization of the Ehrlich pathway into mitochondria increased isobutanol production by 260%, whereas overexpression of the same pathway in the cytoplasm only improved yields by 10%, compared with a strain overproducing enzymes involved in only the first three steps of the biosynthetic pathway. Subcellular fractionation of engineered strains revealed that targeting the enzymes of the Ehrlich pathway to the mitochondria achieves greater local enzyme concentrations. Other benefits of compartmentalization may include increased availability of intermediates, removing the need to transport intermediates out of the mitochondrion and reducing the loss of intermediates to competing pathways.

Metabolic engineering of cytoplasmic biosynthetic pathways to create industrial strains of *S. cerevisiae* is commonplace, whereas engineering of biosynthetic pathways that function in mitochondria has largely been ignored. Yet mitochondria have many potential advantages for metabolic engineering, including the sequestration of diverse metabolites, such as heme, tetrahydrofolate, ubiquinone,  $\alpha$ -ketoacids, steroids, aminolevulinic acid, biotin and lipoic acid<sup>1–15</sup>. In addition, mitochondria contain intermediates of many central metabolic pathways, including the tricarboxylic acid (TCA) cycle, amino-acid biosynthesis and fatty-acid metabolism<sup>3,8,16,17</sup>.

The environment in the mitochondrial matrix differs from that in the cytoplasm: it has higher pH, lower oxygen concentration and a more reducing redox potential<sup>18–20</sup>. This environment may more closely match the optimal for maximal activity of many enzymes such as the iron-sulfur clusters (ISCs), which are essential cofactors of enzymes in diverse pathways including branched-chain amino acid and isoprenoid biosynthetic pathways, and which are synthesized exclusively in mitochondria<sup>21</sup>. Although ISCs can be exported to the cytoplasm, the molecular machinery that loads ISCs onto extramitochondrial enzymes is likely to be incompatible with most exogenous ISC apoenzymes, especially those of bacterial or archaeal origin<sup>22,23</sup>. The smaller volume of mitochondria could concentrate substrates favoring faster reaction rates and productivity, and confine metabolic intermediates, avoiding repressive regulatory responses, diversion of intermediates into competing pathways or even toxic effects of intermediates to cytoplasmic or nuclear processes.

To take advantage of the potential attributes of the mitochondrial environment, we engineered yeast mitochondria to produce three

advanced biofuels: isobutanol, isopentanol and 2-methyl-1-butanol (collectively called fusel alcohols). Isobutanol is synthesized in yeast by the valine Ehrlich degradation pathway<sup>24</sup> but can also be produced from pyruvate in a biosynthetic pathway that recruits the upstream pathway of valine biosynthesis (Fig. 1). The upstream isobutanol pathway, between pyruvate and  $\alpha$ -ketoisovalerate ( $\alpha$ -KIV), comprises acetolactate synthase (ALS; encoded by *ILV2*), ketol-acid reductoisomerase (KARI; encoded by *ILV5*) and dehydroxyacid dehydratase (DADH; encoded by *ILV3*) (Fig. 1). The downstream isobutanol pathway comprises  $\alpha$ -ketoacid decarboxylase ( $\alpha$ -KDC) and alcohol dehydrogenase (ADH).

The complete biosynthetic pathway for isobutanol production has been engineered in bacteria<sup>25–30</sup>. In yeast, the isobutanol biosynthetic pathway is complicated by subcellular compartmentalization: the upstream part of the pathway is confined to mitochondria<sup>3</sup>, whereas the downstream part of the pathway is confined to the cytoplasm (Ehrlich pathway<sup>24</sup>; Fig. 1a). Therefore the simple overexpression of all the enzymes in the isobutanol pathway could create a substantial bottleneck in which the transport of intermediates across membranes reduces productivity and enables these intermediates to be consumed by competing pathways. Nevertheless, the isobutanol pathway has been partially constructed in yeast, by overexpressing only some of the enzymes, and in their natural compartments, to increase isobutanol production<sup>31–33</sup>. Although efforts have been made to transfer the isobutanol pathway, partly or completely, to either compartment<sup>34</sup> (upstream to cytoplasm<sup>35,36</sup> or downstream to mitochondria<sup>37,38</sup>), there has been no direct comparison of the effects of mitochondrial versus cytoplasmic engineering of downstream enzymes in fully assembled pathways.

<sup>1</sup>Department of Chemical Engineering, Massachusetts Institute of Technology, Cambridge, Massachusetts, USA. <sup>2</sup>Whitehead Institute for Biomedical Research, Cambridge, Massachusetts, USA. Correspondence should be addressed to G.R.F. (gfink@wi.mit.edu) or G.S. (gregstep@mit.edu).

Received 16 November 2012; accepted 11 January 2013; published online 17 February 2013; doi:10.1038/nbt.2509

Yeast mitochondria have been exploited through gene targeting to produce hydrocortisone<sup>39</sup> and plant terpenoids<sup>40</sup>; however, these pathways were split across multiple subcellular compartments. In this study we engineered strains with complete isobutanol pathways targeted to mitochondria (all enzymes in the pathway were overexpressed in mitochondria) to avoid pathway subcompartmentalization (Fig. 1b) and compared their fusel alcohol production with that in strains in which all enzymes of the isobutanol pathway are overexpressed in their natural compartments (divided into an upstream mitochondrial and downstream cytoplasmic pathways; Fig. 1a). Moving the complete pathway into a single compartment (mitochondria) resulted in a substantial increase in the production of fusel alcohols, and we provide evidence that this increase is at least partly due to a higher availability of the key  $\alpha$ -KIV intermediate and increased local enzyme concentrations resulting from mitochondrial compartmentalization.

To reconstruct multiple isoforms of the isobutanol pathway, we developed a standard, flexible set of vectors (pJLA vector series) that facilitates targeting of identical pathways to either the cytoplasm or mitochondria. These new tools enabled rapid assembly and comparison of eighteen isoforms (or 'isopathways') of the complete isobutanol pathway, in which their downstream enzymes are targeted to either the mitochondria or the cytoplasm, but are in every other way identical. This approach enabled us to measure the effect of mitochondrial engineering of isobutanol pathways for the production of isobutanol, isopentanol and 2-methyl-1-butanol.

## RESULTS

### Construction of partial and complete isobutanol pathways

We cloned the enzymes required for the synthesis of isobutanol using a standardized vector series (pJLA vectors) that we developed for gene overexpression in *S. cerevisiae* (Online Methods). This tool facilitated the assembly of multiple isobutanol isopathways, into single high-copy (2 $\mu$ ) plasmids, such that each isopathway was introduced into yeast on a single vector.

We targeted the downstream enzymes to either the cytoplasm or mitochondria (Fig. 1), using the N-terminal mitochondrial localization signal from subunit IV of the yeast cytochrome *c* oxidase (CoxIV)<sup>41</sup> (Supplementary Tables 1 and 2). The parallel assembly of cytoplasmic and mitochondrial pathways using pJLA vectors allows for the overexpression of pathways and enzymes that are identical except for the subcellular compartment to which these enzymes are targeted (aside from a single N-terminal glutamine in enzymes targeted to mitochondria<sup>41</sup>).

We prepared multigenic plasmids containing partial or complete isobutanol pathways (Supplementary Tables 1 and 2), each with the same upstream pathway composed of the endogenous *ILV2*, *ILV3* and *ILV5* (*ILV* genes), driven by the *TDH3*, *PGK1* and *TEF1* promoters, respectively. We constructed partial isobutanol pathways by adding to the upstream pathway construct one of three possible  $\alpha$ -KDCs (LIKivd from *L. lactis*, *KID1* or *ARO10*, both from *S. cerevisiae*) driven by the *TDH3* promoter and targeted to mitochondria. Complete isobutanol pathway constructs contained, in addition to the upstream pathway, one of the three  $\alpha$ -KDCs driven by the *TDH3* promoter, and one of three possible ADHs (*ADH7* from *S. cerevisiae*, EcFucO from *Escherichia coli* or LIAdhA<sup>RE1</sup>, a variant with increased affinity to isobutyraldehyde, from *Lactococcus lactis*<sup>26</sup>) driven by the *TEF1* promoter; with both downstream enzymes targeted to either mitochondria or the cytoplasm. This assembly produced a total of 4 partial and 18 complete isobutanol pathway constructs (Online Methods and Supplementary Note).

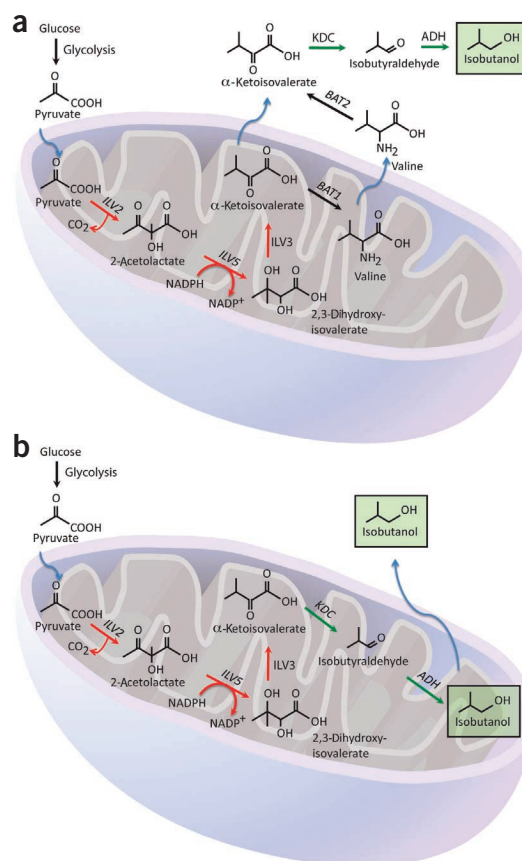


**Figure 1** Isobutanol pathways. (a) The upstream pathway (composed of *ILV2*, *ILV5* and *ILV3*) is part of the valine biosynthetic pathway (red arrows), whereas the downstream pathway (composed of *KDC* and *ADH*) is the Ehrlich valine degradation pathway (green arrows). The  $\alpha$ -KIV intermediate is interconverted to valine by *BAT1* and *BAT2*. The upstream and downstream pathways are naturally separated between the mitochondria and cytoplasm, respectively. (b) The engineered pathway results in targeting of the complete pathway to the mitochondrial compartment. Blue arrows depict transport across mitochondrial membranes.

### Overexpression of the isobutanol pathway components

We transformed plasmids with partial or complete isobutanol pathways into yeast (Supplementary Table 3) and compared the average isobutanol titers obtained in 24-h high-cell-density fermentations in minimal medium from the various isobutanol isopathways (Online Methods and Fig. 2a). Greater isobutanol titers reflect greater isobutanol productivity per yeast cell (specific titers; Fig. 2b), and this effect was reproducible (strains had stable productive phenotypes after being stored at 4 °C or -80 °C, with  $n \geq 3$ ).

The incremental addition of each component of the isobutanol pathway resulted in cumulative increases in isobutanol production in high-cell-density fermentations but only if the downstream enzymes are targeted to mitochondria (Fig. 2a,b), suggesting that these downstream enzymes are active in mitochondria. The background isobutanol production of yeast transformed with an empty plasmid (strain JAy2) in 24-h high-cell-density fermentations in minimal medium was 28 mg l<sup>-1</sup>  $\pm$  2 mg l<sup>-1</sup> ( $\pm$  s.d.). When we overexpressed the products of upstream *ILV* genes (JAY38), isobutanol production increased approximately fivefold, to 136 mg l<sup>-1</sup>  $\pm$  23 mg l<sup>-1</sup>. The additional overexpression of the first downstream enzyme ( $\alpha$ -KDC), targeted to mitochondria in strains JAY49, JAY51 and JAY53,

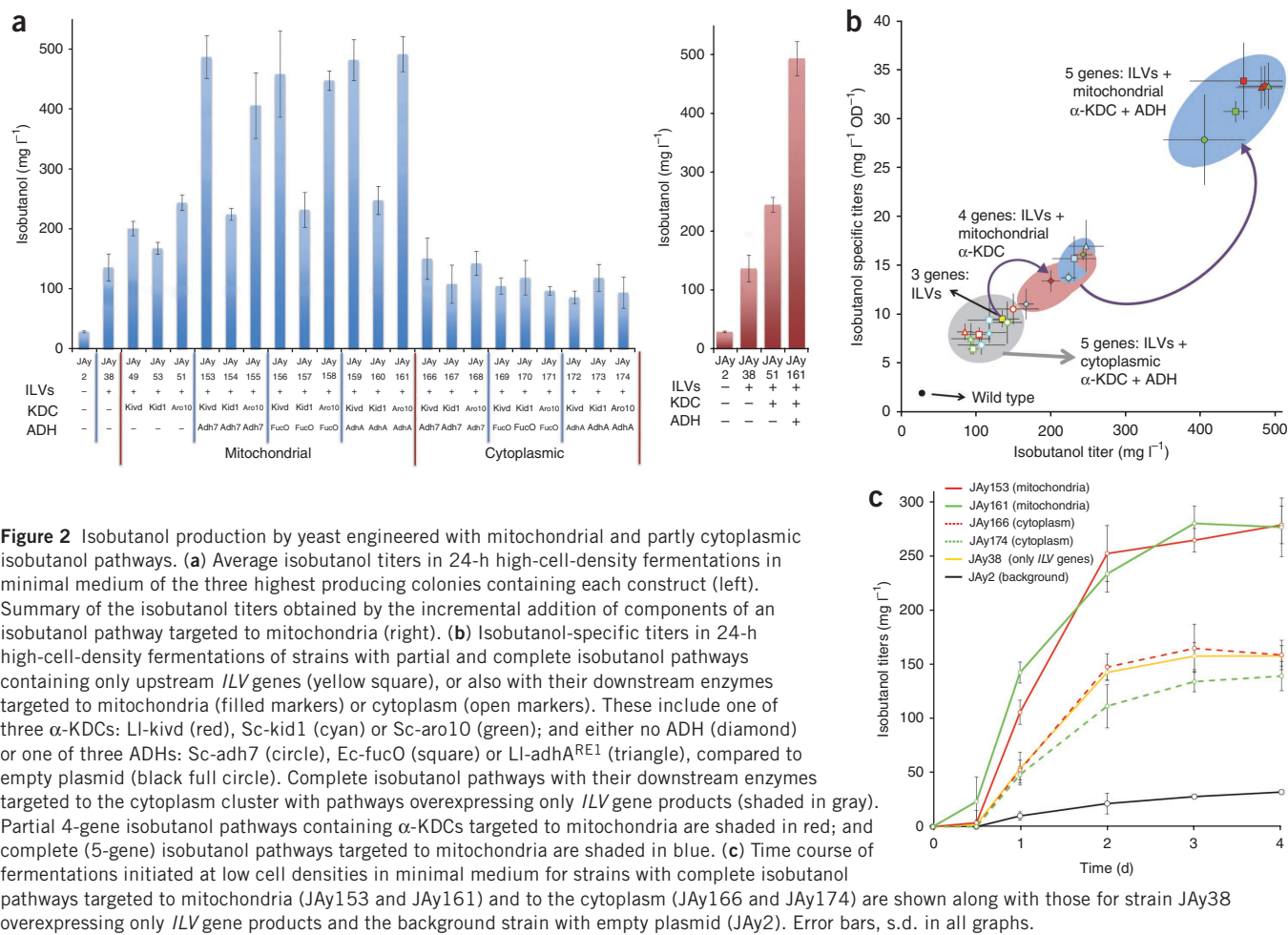


**Figure 2** Isobutanol production by yeast engineered with mitochondrial and partly cytoplasmic isobutanol pathways. **(a)** Average isobutanol titers in 24-h high-cell-density fermentations in minimal medium of the three highest producing colonies containing each construct (left). Summary of the isobutanol titers obtained by the incremental addition of components of an isobutanol pathway targeted to mitochondria (right). **(b)** Isobutanol-specific titers in 24-h high-cell-density fermentations of strains with partial and complete isobutanol pathways containing only upstream *ILV* genes (yellow square), or also with their downstream enzymes targeted to mitochondria (filled markers) or cytoplasm (open markers). These include one of three  $\alpha$ -KDCs: Li-kivd (red), Sc-kid1 (cyan) or Sc-aro10 (green); and either no ADH (diamond) or one of three ADHs: Sc-adh7 (circle), Ec-fucO (square) or Li-adh<sup>ARE1</sup> (triangle), compared to empty plasmid (black full circle). Complete isobutanol pathways with their downstream enzymes targeted to the cytoplasm cluster with pathways overexpressing only *ILV* gene products (shaded in gray). Partial 4-gene isobutanol pathways containing  $\alpha$ -KDCs targeted to mitochondria are shaded in red; and complete (5-gene) isobutanol pathways targeted to mitochondria are shaded in blue. **(c)** Time course of fermentations initiated at low cell densities in minimal medium for strains with complete isobutanol pathways targeted to mitochondria (JAY153 and JAY161) and to the cytoplasm (JAY166 and JAY174) are shown along with those for strain JAY38 overexpressing only *ILV* gene products and the background strain with empty plasmid (JAY2). Error bars, s.d. in all graphs.

resulted in isobutanol titers as high as  $244 \text{ mg l}^{-1} \pm 13 \text{ mg l}^{-1}$  in JAY51, almost double the production from overexpression of the *ILV* gene products alone (JAY38). The overexpression of the complete mitochondria-targeted isobutanol pathway (by adding ADHs targeted to mitochondria in strains JAY153–JAY161) resulted in isobutanol titers as high as  $486 \text{ mg l}^{-1} \pm 36 \text{ mg l}^{-1}$  and  $491 \text{ mg l}^{-1} \pm 29 \text{ mg l}^{-1}$  in JAY153 and JAY161, respectively, which is an additional twofold increase from the four-gene isobutanol pathway and almost 18-fold increase from JAY2 (the control strain harboring an empty plasmid). By contrast, yeast overexpressing the downstream  $\alpha$ -KDCs and ADHs targeted to the cytoplasm (strains JAY166–JAY174) produced isobutanol titers of only  $151 \text{ mg l}^{-1} \pm 34 \text{ mg l}^{-1}$  in JAY166, similar to the titers produced in JAY38, which overexpresses only the products of upstream *ILV* genes in mitochondria (Fig. 2a,b).

We also replicated the superiority of mitochondrial isobutanol production compared with cytoplasmic isobutanol production in fermentations initiated at low cell densities (OD of 0.03) both in minimal and complete media (Fig. 2c, Supplementary Table 4 and Online Methods). The strains overexpressing mitochondria-targeted enzymes of isobutanol downstream pathways, JAY153 and JAY161, outperformed JAY166 and JAY174 in which the same genes products were overexpressed in the cytoplasm, with isobutanol titers as high as  $279 \text{ mg l}^{-1} \pm 16 \text{ mg l}^{-1}$  and  $635 \text{ mg l}^{-1} \pm 23 \text{ mg l}^{-1}$  in minimal and complete media, respectively. Strains JAY166 and JAY174, which overexpress the same downstream enzymes of isobutanol pathways in the cytoplasm, had titers similar to those obtained with JAY38

(overexpressing only the products of *ILV* genes in mitochondria), which reached  $157 \text{ mg l}^{-1} \pm 12 \text{ mg l}^{-1}$  of isobutanol in minimal medium, and  $384 \text{ mg l}^{-1} \pm 15 \text{ mg l}^{-1}$  in complete medium. By contrast, strain JAY2 (with empty plasmid) produced only  $28 \text{ mg l}^{-1} \pm 1 \text{ mg l}^{-1}$  and  $67 \text{ mg l}^{-1} \pm 10 \text{ mg l}^{-1}$  of isobutanol in minimal and complete media, respectively (Fig. 2c and Supplementary Table 4).

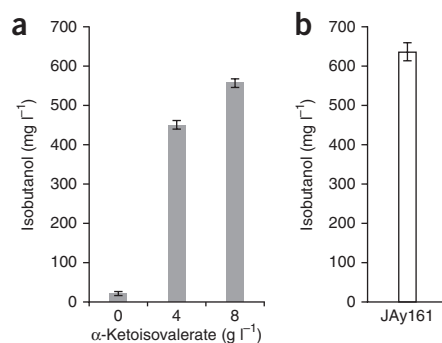


**Figure 3** The effect of cytoplasmic  $\alpha$ -ketoisovalerate on isobutanol production. **(a)** Cytoplasmic isobutanol production of a strain overexpressing Li-kivd targeted to the cytoplasm, with or without addition of the  $\alpha$ -ketoisovalerate intermediate to the culture medium. **(b)** Isobutanol production in strain JAY161 (which has a mitochondria-targeted pathway) without adding  $\alpha$ -ketoisovalerate **(b)**. Error bars, s.d. in all graphs.

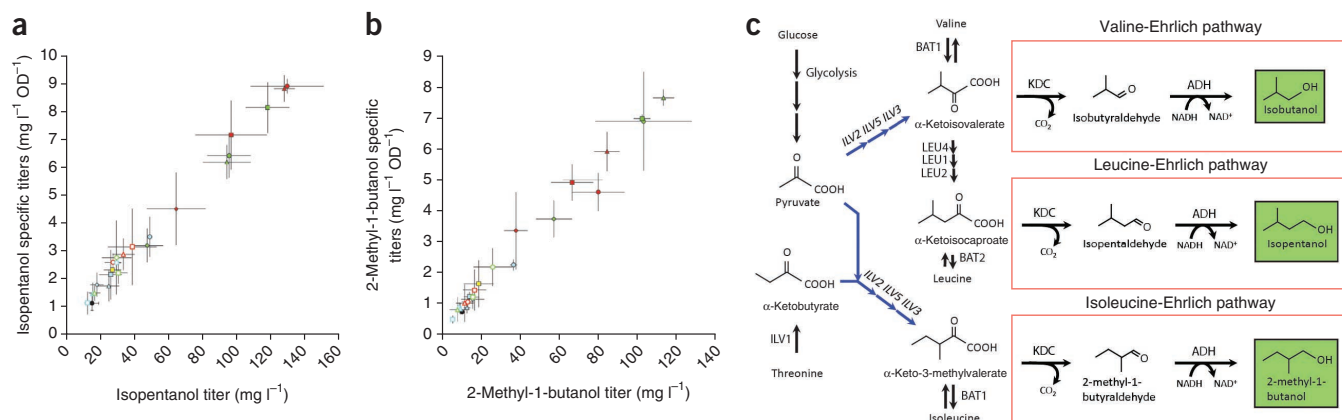


**Figure 4** Production of isopentanol and 2-methyl-1-butanol. **(a,b)** Specific titers of isopentanol **(a)** and 2-methyl-1-butanol **(b)** obtained in 24-h high-cell-density fermentations in minimal medium. The plots show the average titers of the three highest producing strains of each alcohol, for each construct. The constructs include partial and complete isobutanol pathways containing only upstream *ILV* genes (yellow square), or also with their downstream enzymes targeted to mitochondria (filled markers) or cytoplasm (open markers). These include one of three  $\alpha$ -KDCs: LI-kivd (red), Sc-kid1 (cyan) or Sc-aro10 (green); and either no ADH (diamond), or one of three ADHs: Sc-adh7 (circle), Ec-fucO (square) or LI-adhARE1 (triangle), compared to empty plasmid (black full circle). **(c)** The isobutanol, isopentanol and 2-methyl-1-butanol biosynthetic pathways, showing considerable overlap in the upstream pathways (blue arrows) and identical downstream, Ehrlich degradation pathways (red boxes). Error bars, s.d. in all graphs.

To determine whether increased availability of  $\alpha$ -KIV in mitochondria has a substantial role in improving the performance of those pathways that we targeted to the mitochondria, we tested whether increasing the cytoplasmic availability of  $\alpha$ -KIV, by adding this intermediate to the culture medium, has an effect on cytoplasmic isobutanol production. Increased availability of  $\alpha$ -KIV in the cytoplasm increased isobutanol production of strains overexpressing  $\alpha$ -KDCs in the cytoplasm (Fig. 3a), achieving titers that approached those obtained with strains engineered with mitochondrial isobutanol pathways (Fig. 3b). This indicates that  $\alpha$ -KIV is normally a limiting intermediate in the cytoplasm and that downstream enzymes targeted to mitochondria likely benefit from an increased availability of  $\alpha$ -KIV in this organelle.

#### Mitochondrial production of other branched-chain alcohols

Yeast strains with mitochondrial isobutanol pathways also produced substantial amounts of isopentanol (3-methyl-1-butanol) and 2-methyl-1-butanol, compared with strains overexpressing complete isobutanol pathways but with cytoplasmic downstream enzymes (Fig. 4). The average isopentanol and 2-methyl-1-butanol titers in 24-h high-cell-density fermentations of strains with the different isobutanol constructs exhibited a pattern similar to the one observed for isobutanol production (Fig. 4a,b). In fermentations initiated at low cell densities, overexpressing the products of *ILV* genes alone (JAY38) or with cytoplasmic downstream pathways (JAY166 and JAY174) had little

to no measurable effect on isopentanol and 2-methyl-1-butanol production. However, we achieved measurable increases in the production of both alcohols when enzymes of complete isobutanol pathways were overexpressed in mitochondria (Supplementary Table 4).

Overexpression of the products of *ILV* genes alone (JAY38) in high-cell-density fermentations resulted in modest increases in the production of isopentanol ( $28 \pm 5$  mg l<sup>-1</sup>) and 2-methyl-1-butanol ( $19 \pm 8$  mg l<sup>-1</sup>), compared with that in strain JAY2, which harbors an empty plasmid ( $16 \pm 4$  mg l<sup>-1</sup> and  $11 \pm 1$  mg l<sup>-1</sup>, respectively; Fig. 4a,b). The addition of plasmids encoding  $\alpha$ -KDCs targeted to mitochondria additionally increased the production of these alcohols to as high as  $65$  mg l<sup>-1</sup>  $\pm$   $17$  mg l<sup>-1</sup> of isopentanol in JAY49 and  $57$  mg l<sup>-1</sup>  $\pm$   $9$  mg l<sup>-1</sup> of 2-methyl-1-butanol in JAY51. When we targeted both  $\alpha$ -KDCs and ADHs to mitochondria, we obtained titers as high as  $130$  mg l<sup>-1</sup>  $\pm$   $21$  mg l<sup>-1</sup> and  $113$  mg l<sup>-1</sup>  $\pm$   $5$  mg l<sup>-1</sup> of isopentanol and 2-methyl-1-butanol in JAY153 and JAY161, respectively, which

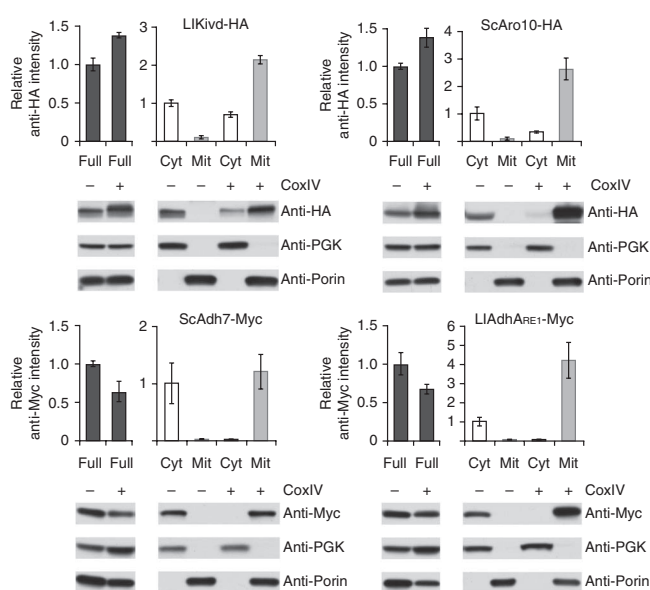


**Figure 5** Effects of the CoxIV mitochondrial localization signal on the cellular localization and local concentration of targeted enzymes. Subcellular distribution of  $\alpha$ -KDCs and ADHs fused to hemagglutinin (HA) or Myc tags, respectively, and targeted to the cytoplasm (no CoxIV) or mitochondria (via CoxIV). Gels were loaded with 20  $\mu$ g of total protein from cytoplasmic (Cyt) or mitochondrial (Mit) fractions; or equal amounts of complete cells (Full). Densitometry measurements of cytoplasmic and mitochondrial fractions were normalized relative to signals of enzymes targeted to the cytoplasm. Densitometry measurements of full cell samples were normalized to signals from strains with enzymes targeted to the cytoplasm. As controls, the distributions of PGK and porin, which are specific markers for the cytoplasmic and mitochondrial fractions, respectively, were determined on the same blots. Error bars, s.d.

represent approximately 8-fold and 11-fold increases in titers relative to the strain containing the empty plasmid, respectively. In contrast, pathways with the same downstream enzymes targeted to cytoplasm produced only  $28 \text{ mg l}^{-1} \pm 5 \text{ mg l}^{-1}$  of isopentanol (JAY166), which is indistinguishable from overexpressing the upstream pathway alone (JAY38), and  $8 \text{ mg l}^{-1} \pm 4 \text{ mg l}^{-1}$  of 2-methyl-1-butanol (JAY174), which is indistinguishable from background (JAY2) (Fig. 4a,b).

### Increased concentrations of mitochondria-targeted enzymes

To ensure that the CoxIV mitochondrial localization signal targeted enzymes to mitochondria, we quantified the amount of targeted enzymes in subcellular fractionations of our engineered strains. We detected all enzymes fused to the CoxIV mitochondrial localization signal in the mitochondrial fractions, whereas we detected enzymes lacking the CoxIV signal only in cytoplasmic fractions (Fig. 5). Furthermore, three of the four enzymes analyzed exhibited increased local concentrations in mitochondria, compared to cytoplasm (overexpressed under the same promoter), reaching as much as a fourfold increase in Ll-adhA<sup>RE1</sup> concentration when targeted to mitochondria. These results confirm not only that the CoxIV mitochondrial localization signal is an effective signal to target the enzymes in this study to mitochondria, but also that it is possible to achieve higher local enzyme concentrations through targeting to this organelle, probably owing to the smaller volume of mitochondria compared to the cytoplasm.

### DISCUSSION

Our results show that targeting the entire isobutanol pathway to mitochondria greatly improved the titers, yields and productivities of branched-chain alcohols, compared to production in the cytoplasm. Isobutanol production increased substantially when we targeted overexpressed downstream enzymes ( $\alpha$ -KDC and ADH) to mitochondria rather than to the cytoplasm. To measure the effect of targeting enzymes to mitochondria, we analyzed isobutanol titers obtained in high-cell-density fermentations in minimal medium when downstream enzymes, supplementing the overexpression of products of *ILV* genes, were targeted to either mitochondria or the cytoplasm. JAY153 (with mitochondrial Ll-kivd and Sc-adh7) produced  $486 \text{ mg l}^{-1} \pm 36 \text{ mg l}^{-1}$  of isobutanol, whereas JAY166 (with the same downstream enzymes targeted to cytoplasm) produced  $151 \text{ mg l}^{-1} \pm 34 \text{ mg l}^{-1}$ . As JAY38 (in which only products of the *ILV* genes were overexpressed) produced  $136 \text{ mg l}^{-1} \pm 23 \text{ mg l}^{-1}$  of isobutanol, the effect of targeting Ll-kivd and Sc-adh7 to mitochondria was an approximately 260% improvement in isobutanol titers, as opposed to a maximum improvement of 10% with the same enzymes targeted to the cytoplasm (JAY166 isobutanol titers were the highest of all strains overexpressing cytoplasmic downstream enzymes).

Our combinatorial constructs permitted a rapid comparison of the efficacy of native and heterologous enzymes for isobutanol production. The choice of decarboxylase in the downstream isobutanol pathway produced considerable effects, whereas the activity of the three selected dehydrogenases was roughly equivalent. The specific  $\alpha$ -KDC homolog used has an important impact on titers of isobutanol, with Ll-kivd and Sc-aro10 being substantially more active than Sc-kid1. By contrast, the three ADHs selected in this study were roughly equally active, despite the reported NADPH dependence of Sc-adh7 (ref. 42), the improved affinity for isobutyraldehyde of Ll-adhA<sup>RE1</sup> (ref. 26) and the ability of Ec-fucO to reduce relatively large aldehydes<sup>43</sup>.

Isopentanol and 2-methyl-1-butanol titers also increased in strains containing mitochondrial isobutanol pathways. These increased titers are likely due to (i) overexpression of the upstream *ILV* gene products (*ILV2*, *ILV3* and *ILV5*), also involved in the biosynthetic pathways

of leucine and isoleucine, resulting in the production of the relevant  $\alpha$ -ketoacids ( $\alpha$ -ketoisocaproate and  $\alpha$ -keto-3-methylvalerate, respectively; Fig. 4c); (ii) the two  $\alpha$ -ketoacid precursors to these alcohols being suitable substrates for the overexpressed  $\alpha$ -KDCs, with Ll-kivd having a bias for isopentanol production, Sc-aro10 having higher activity for 2-methyl-1-butanol production and Sc-kid1 with no detectable activity; and (iii) the aldehydes they produce being potential substrates for the three overexpressed ADHs, which have no apparent preference for the production of either alcohol (Fig. 4 and Supplementary Table 4).

Similar to the case with isobutanol production, overexpression of  $\alpha$ -KDCs and ADHs increased the production of isopentanol and 2-methyl-1-butanol but only when these enzymes were targeted to mitochondria. Moreover, the effects of mitochondrial targeting on the production of isopentanol and 2-methyl-1-butanol in high-cell-density fermentations were even larger than those observed for isobutanol. Overexpression of downstream enzymes of the isobutanol pathway in mitochondria increased isopentanol and 2-methyl-1-butanol titers (from the overexpression of *ILV* gene products alone) by as much as 370% and 500%, respectively. In the case of 2-methyl-1-butanol (as with isobutanol), this was probably due to the fact that its  $\alpha$ -ketoacid precursor,  $\alpha$ -keto-3-methylvalerate, is synthesized in mitochondria, and thus has higher availability in this organelle. However, the case of isopentanol is paradoxical because its  $\alpha$ -ketoacid precursor,  $\alpha$ -ketoisocaproate, is synthesized in the cytoplasm. It is possible that mitochondrial pathways, by consuming  $\alpha$ -ketoisovalerate in mitochondria, mitigate the repression that *ILV* gene product overexpression is likely to effect on  $\alpha$ -ketoisocaproate biosynthesis (and thus isopentanol production), owing to the tight regulation of leucine biosynthesis<sup>3</sup>.

Mitochondrial targeting offers a more frugal way to direct metabolic flux toward isobutanol production, compared with other possible isobutanol pathway configurations. Pathways in which the downstream enzymes are expressed in the cytoplasm, and separated from the mitochondrial upstream pathway (as in strains JAY166–JAY174), might benefit from the overexpression of branched-chain amino acid aminotransferases (*BAT1* and *BAT2*, Fig. 1a), as suggested by the overexpression of cytoplasmic *BAT2* (ref. 31). However, to exploit the increased abundance of  $\alpha$ -ketoisovalerate provided by the upstream pathway in this configuration, it would be necessary to overexpress at least one, and most likely two additional genes (*BAT1* and *BAT2*), compared to fully mitochondrial pathways. This not only increases the engineering burden, but also increases the chances of off-target effects, such as the possibility of overproducing valine as a side product. Thus, mitochondrial engineering offers a more efficient way to direct the increased metabolic flux provided by overexpressed *ILV* gene products toward isobutanol, without invoking valine as an intermediate.

Expression of the complete isobutanol pathway in the cytoplasm by overexpression of gene products of *ILV2*, *ILV3* and *ILV5* simply

**Table 1** Highest titers, yields and productivities achieved with JAY161

JAY161	Isobutanol <sup>a</sup>	Isopentanol <sup>b</sup>	2-Methyl-1-butanol <sup>b</sup>	Total fusel alcohols
Titer <sup>c</sup> (mg l <sup>-1</sup> )	635 ± 23	95 ± 12	118 ± 28	850 ± 60
Yield <sup>c</sup> (mg per g glucose)	6.4 ± 0.2	1.0 ± 0.1	1.1 ± 0.2	8.5 ± 0.5
Productivity <sup>d</sup> (mg l <sup>-1</sup> h <sup>-1</sup> )	20.5 ± 1.2	4.0 ± 0.6	4.7 ± 0.2	29 ± 2

<sup>a</sup>The highest isobutanol production levels previously reported<sup>35</sup> are: titer,  $630 \pm 14 \text{ mg l}^{-1}$ ; yield,  $14.9 \pm 0.6 \text{ mg per g glucose}$ ; and productivity (calculated),  $6.6 \pm 0.1 \text{ mg l}^{-1} \text{ h}^{-1}$ . These values correspond to fermentations in which valine was excluded from the medium, as this nutrient inhibits isobutanol production of their strains. <sup>b</sup>Overproduction of isopentanol or 2-methyl-1-butanol in engineered yeast has not been previously reported to our knowledge. <sup>c</sup>Obtained in low-cell-density fermentations in complete medium. <sup>d</sup>Obtained in 24-h high-cell-density fermentations in minimal medium.

lacking mitochondrial localization signals does not increase isobutanol production<sup>33,35,36</sup>. Increased isobutanol production in the cytoplasm might be achieved by other means but involves, among other things, modifications of upstream enzymes, overexpression of native and heterologous ISC assembly and insertion machineries (to obtain cytosolically active *ILV3* gene product homologs), and overexpression of multiple native and heterologous chaperones<sup>36</sup>, or removal of the native branched-chain amino acid biosynthetic pathway<sup>35</sup>. These numerous manipulations contrast with the modest changes required to achieve an approximately fivefold increase in isobutanol production by overexpressing the native *ILV* gene products in their natural environment of mitochondria; and an almost 18-fold increase that can be achieved by also targeting the downstream enzymes to mitochondria (obtained in high-cell-density fermentations).

The titers, yields and productivities of isopentanol and 2-methyl-1-butanol we achieved (Table 1) with JAY161, are the highest ever reported in yeast to our knowledge. The isobutanol productivity we observed is more than double the highest reported in the literature<sup>35</sup>, and our titers were as high as the highest ones reported, but our strains required higher sugar concentrations. Furthermore, our strains produced substantial yields of isobutanol in complete medium containing valine, whereas engineering the complete pathway for overexpression in the cytoplasm rendered it sensitive to inhibition by valine<sup>35</sup>, a nutrient that is likely to be present in industrial feedstocks. Although these alcohols are known to be toxic, even our best isobutanol producers did not show any reduced fitness, measured by growth rate or maximal cellular density. The challenge to further improve yields, titers and productivities will require diverting more carbon flux, from ethanol to production of branched-chain alcohols<sup>32,44</sup>.

The strategy of organelle targeting has been applied in plants, where portions of the isoprenoid pathway have been targeted to plastids of the tobacco plant<sup>45</sup>. Unlike in our study, the pathways compared in tobacco plant cytoplasm (mevalonate pathway) and chloroplast (methylerythritol pathway) were not identical, and only their downstream enzymes were overexpressed. Nevertheless, the targeting of a metabolic pathway to the plant plastid, as with our redirection of the isobutanol pathway to yeast mitochondria, resulted in marked increases in the production of desired end products. The sequestration of the isoprenoid pathway in plastids, in common with the confinement of the isobutanol pathway to mitochondria in yeast, might benefit from higher concentrations of enzymes, substrates and cofactors, which would favor higher productivities.

We showed that for isobutanol production in yeast, sequestration of the pathway in the mitochondrion resulted in higher enzyme concentrations, probably owing to their confinement in the relatively smaller volume of the mitochondrial compartment. Moreover, the key  $\alpha$ -KIV intermediate is limiting in the cytosol, but not in mitochondria; thus, targeting the full pathway to mitochondria benefits from increased  $\alpha$ -KIV availability, eliminates the bottleneck of exporting  $\alpha$ -KIV to the cytoplasm and reduces the loss of  $\alpha$ -KIV to competing reactions. Pathways targeted to mitochondria may be additionally enhanced by mutagenesis.

Pathways that are naturally cytoplasmic might also benefit from mitochondrial compartmentalization, because the confinement of enzymes and metabolites to subcellular compartments may result not only in an increase in their local concentrations and proximities but also in the ability to reduce the toxicity of pathway intermediates, bypass inhibitory regulatory networks or avoid competing pathways. Thus, subcellular metabolic engineering has the potential to provide multiple mechanisms to improve the performance of engineered pathways.

## METHODS

Methods and any associated references are available in the [online version of the paper](#).

Note: Supplementary information is available in the [online version of the paper](#).

## ACKNOWLEDGMENTS

We thank K.L. Jones Prather and T.D. Fox for helpful discussions, T.J. Helbig for working on GFP subcellular localization experiments, T. DiCesare for preparing figures, S. Lindquist (Whitehead Institute) for strain Y3929, and members of the Stephanopoulos, Fink and Prather laboratories for discussions and advice. J.L.A. is supported by US National Institutes of Health under Ruth L. Kirchstein National Research Service Award 1F32GM098022-01A1. G.R.F. is supported by National Institutes of Health grant GM040266. This work was supported by Shell Global Solutions (US) Inc.

## AUTHOR CONTRIBUTIONS

J.L.A., G.R.F. and G.S. conceived the project, designed the experiments, analyzed the results and wrote the manuscript. J.L.A. designed and made the pJLA vectors, constructed all pathways and strains, and executed all the experiments.

## COMPETING FINANCIAL INTERESTS

The authors declare no competing financial interests.

Published online at <http://www.nature.com/doi/10.1038/nbt.2509>.

Reprints and permissions information is available online at <http://www.nature.com/reprints/index.html>.

- Attardi, G. & Schatz, G. Biogenesis of mitochondria. *Annu. Rev. Cell Biol.* **4**, 289–333 (1988).
- Fukuda, H., Casas, A. & Batlle, A. Aminolevulinic acid: from its unique biological function to its star role in photodynamic therapy. *Int. J. Biochem. Cell Biol.* **37**, 272–276 (2005).
- Kohlhaw, G.B. Leucine biosynthesis in fungi: entering metabolism through the back door. *Microbiol. Mol. Biol. Rev.* **67**, 1–15 (2003).
- Kumar, A. *et al.* Subcellular localization of the yeast proteome. *Genes Dev.* **16**, 707–719 (2002).
- Lange, H., Kispal, G. & Lill, R. Mechanism of iron transport to the site of heme synthesis inside yeast mitochondria. *J. Biol. Chem.* **274**, 18989–18996 (1999).
- Marquet, A., Bui, B.T. & Florentin, D. Biosynthesis of biotin and lipoic acid. *Vitam. Horm.* **61**, 51–101 (2001).
- Neuburger, M., Rebeille, F., Jourdain, A., Nakamura, S. & Douce, R. Mitochondria are a major site for folate and thymidylate synthesis in plants. *J. Biol. Chem.* **271**, 9466–9472 (1996).
- Paltauf, F., Kohlwein, S.D. & Henry, S.A. Regulation and compartmentalization of lipid synthesis in yeast. in *The Molecular and Cellular Biology of the Yeast Saccharomyces* (eds. Jones, E.W., Pringle, J.R. & Broach, J.R.) 415–500 (Cold Spring Harbor Laboratory Press, 1992).
- Pierrel, F. *et al.* Involvement of mitochondrial ferredoxin and para-aminobenzoic acid in yeast coenzyme Q biosynthesis. *Chem. Biol.* **17**, 449–459 (2010).
- Schonauer, M.S., Kastaniotis, A.J., Kursu, V.A., Hiltunen, J.K. & Dieckmann, C.L. Lipoic acid synthesis and attachment in yeast mitochondria. *J. Biol. Chem.* **284**, 23234–23242 (2009).
- Shannon, K.W. & Rabinowitz, J.C. Isolation and characterization of the *Saccharomyces cerevisiae* MIS1 gene encoding mitochondrial C1-tetrahydrofolate synthase. *J. Biol. Chem.* **263**, 7717–7725 (1988).
- Sulo, P. & Martin, N.C. Isolation and characterization of LIP5. A lipote biosynthetic locus of *Saccharomyces cerevisiae*. *J. Biol. Chem.* **268**, 17634–17639 (1993).
- Tran, U.C. & Clarke, C.F. Endogenous synthesis of coenzyme Q in eukaryotes. *Mitochondrion* **7** (suppl. 7), S62–S71 (2007).
- Urban-Grimal, D., Volland, C., Garnier, T., Dehoux, P. & Labbe-Bois, R. The nucleotide sequence of the HEM1 gene and evidence for a precursor form of the mitochondrial 5-aminolevulinic synthase in *Saccharomyces cerevisiae*. *Eur. J. Biochem.* **156**, 511–519 (1986).
- Zhang, S., Sanyal, I., Bulboaca, G.H., Rich, A. & Flint, D.H. The gene for biotin synthase from *Saccharomyces cerevisiae*: cloning, sequencing, and complementation of *Escherichia coli* strains lacking biotin synthase. *Arch. Biochem. Biophys.* **309**, 29–35 (1994).
- Hiltunen, J.K. *et al.* Mitochondrial fatty acid synthesis type II: more than just fatty acids. *J. Biol. Chem.* **284**, 9011–9015 (2009).
- Stryer, L. *Biochemistry*, 4th edn (W.H. Freeman and Company, 1995).
- Hu, J., Dong, L. & Outten, C.E. The redox environment in the mitochondrial intermembrane space is maintained separately from the cytosol and matrix. *J. Biol. Chem.* **283**, 29126–29134 (2008).
- Orji, R., Postmus, J., Ter Beek, A., Brul, S. & Smits, G.J. *In vivo* measurement of cytosolic and mitochondrial pH using a pH-sensitive GFP derivative in *Saccharomyces cerevisiae* reveals a relation between intracellular pH and growth. *Microbiology* **155**, 268–278 (2009).

20. Schnell, N., Krems, B. & Entian, K.D. The PAR1 (YAP1/SNQ3) gene of *Saccharomyces cerevisiae*, a c-jun homologue, is involved in oxygen metabolism. *Curr. Genet.* **21**, 269–273 (1992).
21. Muhlenhoff, U. & Lill, R. Biogenesis of iron-sulfur proteins in eukaryotes: a novel task of mitochondria that is inherited from bacteria. *Biochim. Biophys. Acta* **1459**, 370–382 (2000).
22. Lill, R. & Muhlenhoff, U. Iron-sulfur-protein biogenesis in eukaryotes. *Trends Biochem. Sci.* **30**, 133–141 (2005).
23. Xu, X.M. & Moller, S.G. Iron-sulfur cluster biogenesis systems and their crosstalk. *ChemBioChem* **9**, 2355–2362 (2008).
24. Hazelwood, L.A., Daran, J.M., van Maris, A.J., Pronk, J.T. & Dickinson, J.R. The Ehrlich pathway for fusel alcohol production: a century of research on *Saccharomyces cerevisiae* metabolism. *Appl. Environ. Microbiol.* **74**, 2259–2266 (2008).
25. Atsumi, S., Hanai, T. & Liao, J.C. Non-fermentative pathways for synthesis of branched-chain higher alcohols as biofuels. *Nature* **451**, 86–89 (2008).
26. Bastian, S. *et al.* Engineered ketol-acid reductoisomerase and alcohol dehydrogenase enable anaerobic 2-methylpropan-1-ol production at theoretical yield in *Escherichia coli*. *Metab. Eng.* **13**, 345–352 (2011).
27. Higashide, W., Li, Y., Yang, Y. & Liao, J.C. Metabolic engineering of *Clostridium cellulolyticum* for production of isobutanol from cellulose. *Appl. Environ. Microbiol.* **77**, 2727–2733 (2011).
28. Jia, X., Li, S., Xie, S. & Wen, J. Engineering a metabolic pathway for isobutanol biosynthesis in *Bacillus subtilis*. *Appl. Biochem. Biotechnol.* **168**, 1–9 (2012).
29. Li, S., Wen, J. & Jia, X. Engineering *Bacillus subtilis* for isobutanol production by heterologous Ehrlich pathway construction and the biosynthetic 2-ketoisovalerate precursor pathway overexpression. *Appl. Microbiol. Biotechnol.* **91**, 577–589 (2011).
30. Smith, K.M., Cho, K.M. & Liao, J.C. Engineering *Corynebacterium glutamicum* for isobutanol production. *Appl. Microbiol. Biotechnol.* **87**, 1045–1055 (2010).
31. Chen, X., Nielsen, K.F., Borodina, I., Kielland-Brandt, M.C. & Karhumaa, K. Increased isobutanol production in *Saccharomyces cerevisiae* by overexpression of genes in valine metabolism. *Biotechnol. Biofuels* **4**, 21 (2011).
32. Kondo, T. *et al.* Genetic engineering to enhance the Ehrlich pathway and alter carbon flux for increased isobutanol production from glucose by *Saccharomyces cerevisiae*. *J. Biotechnol.* **159**, 32–37 (2012).
33. Lee, W.H. *et al.* Isobutanol production in engineered *Saccharomyces cerevisiae* by overexpression of 2-ketoisovalerate decarboxylase and valine biosynthetic enzymes. *Bioprocess Biosyst. Eng.* **35**, 1467–1475 (2012).
34. Hong, K.K. & Nielsen, J. Metabolic engineering of *Saccharomyces cerevisiae*: a key cell factory platform for future biorefineries. *Cell Mol. Life Sci.* **69**, 2671–2690 (2012).
35. Brat, D., Weber, C., Lorenzen, W., Bode, H.B. & Boles, E. Cytosolic re-localization and optimization of valine synthesis and catabolism enables increased isobutanol production with the yeast. *Saccharomyces cerevisiae*. *Biotechnol. Biofuels* **5**, 65 (2012).
36. Urano, J. *et al.* US patent. US 2011/0076733 A1 (2011).
37. Anthony, L.C., Huang, L.L. & Ye, R.W. US patent. US 2010/0129886 A1 (2010).
38. Buelter, T., Meinhold, P., Smith, C., Aristidou, A., Dundon, C.A. & Urano, J. *World patent*. WO 2010/075504A2 (2010).
39. Szczebara, F.M. *et al.* Total biosynthesis of hydrocortisone from a simple carbon source in yeast. *Nat. Biotechnol.* **21**, 143–149 (2003).
40. Farhi, M. *et al.* Harnessing yeast subcellular compartments for the production of plant terpenoids. *Metab. Eng.* **13**, 474–481 (2011).
41. Maarse, A.C. *et al.* Subunit IV of yeast cytochrome *c* oxidase: cloning and nucleotide sequencing of the gene and partial amino acid sequencing of the mature protein. *EMBO J.* **3**, 2831–2837 (1984).
42. Larroy, C., Pares, X. & Biosca, J.A. Characterization of a *Saccharomyces cerevisiae* NADP(H)-dependent alcohol dehydrogenase (ADHVII), a member of the cinnamyl alcohol dehydrogenase family. *Eur. J. Biochem.* **269**, 5738–5745 (2002).
43. Dellomonaco, C., Clomburg, J.M., Miller, E.N. & Gonzalez, R. Engineered reversal of the beta-oxidation cycle for the synthesis of fuels and chemicals. *Nature* **476**, 355–359 (2011).
44. Feldman, R.M.R. *et al.* US patent. US 2011/8017375 B2 (2011).
45. Wu, S. *et al.* Redirection of cytosolic or plastidic isoprenoid precursors elevates terpene production in plants. *Nat. Biotechnol.* **24**, 1441–1447 (2006).

## ONLINE METHODS

**pJLA vectors.** The challenges to re-engineering a biosynthetic pathway in yeast include the necessity of cloning genes encoding the enzymes required for the multiple steps in the pathway, overexpressing those enzymes, and, for the benefit of mitochondrial engineering, retaining the option to target enzymes to the mitochondrion. To expedite this process, permit the screening of enzymes and promoters, and facilitate the assembly and troubleshooting of engineered pathways, we developed standardized pJLA vectors, for gene expression in *S. cerevisiae*, which are applicable to mitochondrial targeting as well as classical metabolic engineering.

The pJLA vectors, derived from the pRS vectors<sup>46</sup>, contain a uniform multi-cloning sequence array flanked by a variety of promoters and terminators, start and stop codons, and optional in-frame tags (**Supplementary Fig. 1a**). This assembly allows the parallel cloning of genes into any vector of the series to build constructs with different promoters and the option to produce untagged protein, add an N- or C-terminal affinity tag (his, HA or Myc tags), or the CoxIV mitochondrial localization signal.

A second key feature in pJLA vectors is the ability to insert multiple gene expression cassettes into a single plasmid, in tandem or inverted directions, so that an entire metabolic pathway may be introduced into yeast via a single vector (**Supplementary Fig. 1b**). What makes this feasible is a triad of unique restriction sites (XmaI, MreI and AscI) that flank all expression cassettes. This feature allows the sequential insertion of multiple gene expression cassettes into the same plasmid by the iterative ligation of inserts obtained from XmaI-AscI digestions into vectors linearized with MreI and AscI, which produce a tandem insertion, an undigestible XmaI-MreI scar and a new triad of XmaI, MreI and AscI unique sites, available to repeat the reaction for a subsequent insertion. Similar strategies to assemble multiple pieces of DNA have been applied in the BioBricks system<sup>47</sup>. These pJLA vectors have another very useful feature: double digestion of assembled multigenic plasmids with SacI and AscI results in the excision of one DNA fragment per inserted cassette, whose characteristic restriction pattern is diagnostic (**Supplementary Fig. 2**).

A convenient numerical nomenclature (**Supplementary Table 5**) permits the rapid identification of the main features contained in each vector (**Supplementary Note**) and facilitates the naming of vectors derived from future expansions to this series.

**Cloning and screening of isobutanol pathway components.** Initially gene expression cassettes in pJLA vectors were constructed for each individual enzyme (using three possible constitutive promoters and three possible affinity tags, **Supplementary Table 1**). The upstream isobutanol pathway was constructed by cloning the yeast endogenous *ILV2*, *ILV3* and *ILV5* genes in vectors pJLA121<sup>013C3F</sup>, pJLA121<sup>031C1F</sup> and pJLA121<sup>022C2F</sup>, respectively. These vectors lack the engineered CoxIV mitochondrial localization signal of the pJLA series, as these enzymes are naturally targeted to mitochondria (**Fig. 1**).

To test multiple enzymes of the downstream isobutanol pathway (Ehrlich, pathway), we first used vectors pJLA121<sup>021C1F</sup> and pJLA121<sup>121C1F</sup>, which fuse a sequence encoding a C-terminal His tag to genes driven by a *TEF1* promoter and target the gene products to the cytoplasm or mitochondrion, respectively. Using these vectors we screened  $\alpha$ -KDCs and ADHs from various organisms to compare expression in yeast mitochondria and cytoplasm by western blot (**Supplementary Fig. 2a,b**). We also evaluated the increase in isobutanol production obtained with different  $\alpha$ -KDCs overexpressed by themselves, or in combination with the upstream *ILV* gene products, and targeted either to the cytoplasm or to mitochondria (data not shown).

**Construction of a complete mitochondrial or partly cytoplasmic isobutanol pathway.** The screens above, and the known biochemistry of candidate enzymes, informed the selection of three decarboxylases and three dehydrogenases used to build complete isobutanol pathways. The three  $\alpha$ -KDCs we selected are those encoded by *KID1* and *ARO10* from *S. cerevisiae*, both of which have been implicated in the Ehrlich pathway<sup>24</sup>; and Llkivd from *L. lactis*, which has been used in several constructions of the isobutanol biosynthetic pathway<sup>48</sup>. Our selections for dehydrogenases are those encoded by *ADH7* from *S. cerevisiae*, which has also been implicated in fusel alcohol production in yeast<sup>42</sup>, EcfucO from *E. coli*, which has been used in the synthesis of heavy alcohols via the reverse beta-oxidation of fatty acids in bacteria<sup>43</sup>, and

LldhA<sup>RE1</sup> from *L. lactis*, which has been engineered for increased affinity for isobutyraldehyde<sup>26</sup>. These enzymes were selected in the combinatorial assembly of complete isobutanol isopathways with their downstream components targeted to either mitochondria or cytoplasm.

Using the multigenic assembly tool of pJLA vectors, we prepared constructs containing partial or complete isobutanol pathways. The assembly of complete isobutanol pathways using the six selected downstream enzymes in all possible combinations yielded nine mitochondrial constructs and nine cytoplasmic counterparts (**Supplementary Table 2**). We also prepared partial pathways containing the three upstream *ILV* genes (*ILV2*, *ILV3* and *ILV5*), either by themselves, or with genes encoding each of the three selected  $\alpha$ -KDCs targeted to mitochondria.

**Cloning.** The cloning required to develop the pJLA vectors and isobutanol pathways was carried out using the DH5 $\alpha$  strain of *E. coli*. Endogenous genes of the isobutanol pathway (*ILV2*, *ILV3*, *ILV5*, *KID1*, *ARO10* and *ADH7*) were amplified with PCR, using primers containing NheI and XhoI restriction sites, which were used to insert all genes into pJLA vectors. Genes from other organisms were synthesized by Bio Basic Inc., with codons optimized for *S. cerevisiae*. These genes were designed with flanking NheI and XhoI sites at the 5' and 3' ends, respectively (used to insert them into pJLA vectors), and avoiding restriction sites for XmaI, MreI, AscI and other relevant restriction enzymes.

Enzymes were purchased from NEB (SacI, NheI, XbaI, XhoI, KpnI, T4 DNA ligase and Phusion polymerase) or Fermentas (XmaI, AscI, BspEI and MreI), and reactions were carried out following the manufacturers' instructions.

The quality of all vectors was verified before using them for yeast transformation. First we carried out analytical digests of multigenic vectors using SacI and AscI double digestion, which results in the excision of one DNA fragment per inserted cassette (**Supplementary Fig. 2I**), as well as XhoI digestion, which cuts the vector once per inserted cassette (data not shown). The vectors that produced the expected restriction patterns were subsequently sequenced at the Koch Institute Biopolymers and Proteomic Facility at the Massachusetts Institute of Technology.

**Yeast strains and transformations.** The parental strain in this work is the product of mating BY4741 with Y3929, to produce JAY1 (**Supplementary Table 3**). The only auxotrophic marker not complemented by this mating is *ura3 $\Delta$ 0*, which serves as a marker for all vectors used. All yeast transformations for isobutanol production studies were carried out on JAY1, using standard lithium acetate protocols, and the resulting strains are cataloged in **Supplementary Table 3**. Transformation reactions with plasmids containing partial or complete isobutanol pathways resulted in a highly heterogeneous collection of transformants, displaying a wide variability in colony size, growth rates and fusel alcohol productivities. To identify the transformants with the highest fusel alcohol production capabilities, we screened multiple colonies of each transformation in high-cell-density fermentations.

**High-cell-density fermentations.** Single colonies were grown overnight in synthetic complete medium with 2% glucose (without uracil) at 30 °C. The next day, 4 ml of each overnight culture were centrifuged at 2,000g for 3 min, the supernatant was discarded and the cells were resuspended in 10 ml of minimal medium (1 $\times$  YNB) with 10% glucose, in sterile 50-ml conical tubes. Cells were grown in this medium for 12–20 h at 30 °C and 350 r.p.m. agitation, after which they were centrifuged again at 2,000g for 3 min and resuspended in 10 ml of fresh minimal medium with 20% glucose. Fermentations were kept in semiaerobic conditions in the same 50-ml conical tubes, at 30 °C and with shaking at 350 r.p.m. for 24 h. The initial and final optical densities at 600 nm (OD) were averaged to calculate the specific titers of the heavy alcohols. Variations to this protocol, in which fermentations were carried out in 15% glucose, instead of 20%, produced approximately the same heavy-alcohol titers and productivities in all strains tested.

**Fermentations initiated at low cell densities.** Single colonies were grown overnight in 5 ml of synthetic complete medium and 2% glucose (minus uracil) at 30 °C. These overnight cultures were used the next day to inoculate 15 ml of minimal (1 $\times$  YNB) or synthetic complete (minus uracil) media



with 15% or 10% glucose, to an initial OD of 0.03. These fermentations were carried out in sterile 50-ml conical tubes, shaken at 350 r.p.m. and kept at 30 °C for 4 d. Samples were taken at 0 h, 12 h, 1 d, 2 d, 3 d and 4 d to measure their OD as well as concentrations of ethanol, isobutanol, isopentanol and 2-methyl-1-butanol.

**Cytoplasmic isobutanol production from supplemented  $\alpha$ -ketoisovalerate.** To increase the cytoplasmic availability of  $\alpha$ -ketoisovalerate ( $\alpha$ -KIV), this intermediate was added to the fermentation medium. Cells overexpressing an  $\alpha$ -KDC (Ll-kivd) in the cytoplasm were grown overnight in synthetic complete medium (without uracil) with 2% glucose. These cells were used the following day to inoculate to an OD of 0.05, 10 ml of synthetic complete medium (without uracil) with 2% glucose and containing 0 g/l, 4 g/l or 8 g/l of  $\alpha$ -KIV (Sigma). Fermentations were carried out in sterile 50-ml conical tubes, shaken at 350 r.p.m. and kept at 30 °C for 2 d.

**Analysis of heavy alcohols.** The concentrations of heavy alcohols and ethanol were quantified by high-performance liquid chromatography (HPLC), using an Agilent 1100 series instrument. Samples were centrifuged and filtered to remove cells and other solid debris, and analyzed using an Aminex HPX-87H ion-exchange column from Bio-Rad. The column was eluted with 5 mM H<sub>2</sub>SO<sub>4</sub> at 55 °C and 0.75 ml/min for 42 min, which provided adequate separation of all alcohols, including isopentanol from 2-methyl-1-butanol. Alcohols were monitored with a refractive index detector, and their peak areas were compared to those of standard alcohol solutions for quantification.

**Protein blotting, immunodetection and quantification.** To detect expression of tagged protein in full cells by western blot, we collected 1 ml of cells at OD 10.0 (or its equivalent). Cells were centrifuged for 3 min at 2,000g and 4 °C, and the pellets resuspended in 1 ml of 5% trichloroacetic acid solution. After incubating in ice for 10 min, the cells were centrifuged again for 3 min at 2,000g and 4 °C, and the pellets resuspended in 150  $\mu$ l of 10 mM Tris pH 7.5, 1 mM EDTA and 3 mM DTT. Then 150  $\mu$ l of glass beads were added to each tube, and cells were broken on a fastprep cell disrupter (two cycles of 45 s at 6.5 speed setting with a 5-min ice incubation in-between). Finally, 75  $\mu$ l of 3 $\times$  SDS sample buffer was added to each sample. Equal amounts of sample were loaded to polyacrylamide gels (typically 5–15  $\mu$ l), and standard electrophoresis and protein transfer were used to blot proteins on to polyvinylidene fluoride (PVDF) membranes.

For quantitative immunoblotting of subcellular fractions, we isolated the cytoplasmic and mitochondrial fractions of engineered strains, as previously described<sup>49</sup>. We measured the total protein in each subcellular fraction using the Pierce BCA Protein Assay Kit (Thermo Scientific), following the manufacturer's instructions, loaded 20  $\mu$ g of total protein of each subcellular fraction per well of a polyacrylamide gel and after electrophoresis transferred the proteins to PVDF membranes.

Proteins tagged with His, Myc or HA tags were detected using the following antibodies: anti-His6-peroxidase (BMG-His-1, Roche; 1:10,000), anti-c-Myc (9E10, sc-40; Santa Cruz Biotechnology; 1:1,000) and anti-HA-peroxidase, high-affinity (3F10; Roche; 1:100,000), respectively, following the manufacturers' instructions. TAs control for subcellular fractionation experiments, anti-yeast PGK (22C5D8, Invitrogen; 1:10,000) and anti-yeast porin (16G9E6BC4, Invitrogen; 1:20,000) were used, which are specific markers for the cytoplasmic and mitochondrial fractions, respectively. The secondary antibody for detection of c-Myc, anti-PGK or anti-porin was peroxidase-labeled anti-mouse antibody (NA931V, ECL; 1:20,000). The blots were developed using the SuperSignal West Femto developer kit (Thermo Scientific). For quantitative measurements, the Bio-Rad Chemi Doc XRS+ imaging system and Image Lab 3.0.1 software were used to acquire image data, and the ImageJ software was used to quantify luminescence signals by analytical densitometry.

**Protein purification.** Protein purification of some enzymes fused to C-terminal His tags was carried out from cells grown to stationary phase in synthetic complete medium lacking uracil, with 15–20% glucose. Cells were lysed using a SPEX freezer mill, model 6870, and the soluble fraction was run through a Talon metal-affinity resin column, following the manufacturer's instructions.

**Fluorescence microscopy.** To validate the mitochondrial targeting capabilities of pJLA vectors, we used fluorescence microscopy of cells expressing GFP in either mitochondrial or cytoplasmic constructs. To compare the localization of GFP with mitochondria, we used MitoFluor Red 589 (Invitrogen), a red fluorescent dye that specifically stains mitochondria. Cells were incubated in a 1 mM solution of MitoFluor Red 589 at 30 °C for 30 min and washed in PBS before imaging.

Fluorescence microscopy was done with an inverted Nikon TE2000-s microscope equipped with a Spot RT Camera from Diagnostic Instruments. Samples were loaded on glass slides and visualized with a 100 $\times$ , H/N2 oil-immersion objective at room temperature. Green fluorescence (from GFP) was monitored at 500 nm using a HQ:F blocking filter (Nikon). Red fluorescence (MitoFluor Red 589) was monitored at 594 nm with a G-2E/C blocking filter (Nikon). The imaging camera was set to capture 8-bit images that were subsequently processed with Photoshop (Adobe Systems).

46. Christianson, T.W., Sikorski, R.S., Dante, M., Shero, J.H. & Hieter, P. Multifunctional yeast high-copy-number shuttle vectors. *Gene* **110**, 119–122 (1992).
47. Sleight, S.C., Bartley, B.A., Lieviant, J.A. & Sauro, H.M. In-Fusion BioBrick assembly and re-engineering. *Nucleic Acids Res.* **38**, 2624–2636 (2010).
48. Blombach, B. & Eikmanns, B.J. Current knowledge on isobutanol production with *Escherichia coli*, *Bacillus subtilis* and *Corynebacterium glutamicum*. *Bioeng. Bugs* **2**, 346–350 (2011).
49. Gregg, C., Kyrjakov, P. & Titorenko, V.I. Purification of mitochondria from yeast cells. *J. Vis. Exp.* 10.3791/1417 (2009).

## CORRECTION NOTICE

*Nat. Biotechnol.* 31, 335–341 (2013)

---

### Compartmentalization of metabolic pathways in yeast mitochondria improves the production of branched-chain alcohols

Jose L Avalos, Gerald R Fink & Gregory Stephanopoulos

The incorrect version of the supplementary information was posted online and has been replaced as of 3 May 2013.